Time-resolved investigation of laser-induced shape transformation of silver nanoparticles

A. Akin Unal,* A. Stalmashonak, H. Graener,† and G. Seifert
Institut für Physik, Fachgruppe Optik, Martin-Luther-Universität, Hoher Weg 8, 06120 Halle, Germany
(Received 13 May 2009; revised manuscript received 17 August 2009; published 15 September 2009)

Laser-induced permanent shape transformation dynamics of glass-embedded silver nanoparticles is investigated by a pulse-pair irradiation technique, where the nanoparticles are irradiated by pairs of time-delayed femtosecond laser pulses. The temporal evolution of surface plasmon extinction bands is obtained up to a time delay of 1 ns. We find that the aspect ratio of the modified nanoparticles, i.e., the observed dichroism, reduces rapidly to a minimum level within 20 ps after the laser irradiation. From that interpulse delay onward, the resulting aspect ratio stays at that minimum level until 100 ps. Subsequently, for longer time delays, the aspect ratio increases again until 1 ns. Temperature modeling of the nanoparticle-glass system gives evidence that the intermediately reduced dichroism is due to the high diffusion mobility that emitted silver ions can possess within a shell of heated glass around the nanoparticle, in a time window of 100 ps. For longer time delays the size of the heated glass shell gets reduced, thereby limiting the range of ionic diffusion. The theoretical estimations confirm the experimental results and suggest that the nanoparticle shape changes depend strongly on the thermal situation induced to the surrounding glass.

DOI: 10.1103/PhysRevB.80.115415 PACS number(s): 78.67.Bf, 73.20.Mf, 79.20.Ds, 65.80.+n

I. INTRODUCTION

Electron-density waves (i.e., plasmons) in bulk metals are longitudinal waves and do not interact with transverse waves, such as light. However, at metal surfaces the electron and light waves can couple with each other, which results in surface plasmons (SPs). In general, SPs are defined as collective oscillation of conduction-band electrons that occur at a metal-dielectric interface, and they are responsible for specific absorption bands (in the far field)[1] and high local electromagnetic fields (in the near field).[2,3] Depending on the type of the nanostructure and geometry of the interface, SPs can take various forms. In the case of small metal nanoparticles, the SPs are highly localized at the interface of the nanoparticle (NP) and the surrounding dielectric medium.[1]

Upon photon absorption, the energy distribution along the NP happens rather rapidly via electron-electron and electron-phonon interactions—within a few picoseconds.[4,5] The time-resolved investigations of these energy-dissipation mechanisms have been studied mostly in the weak excitation regime, which creates only transient and reversible SP changes.[4–7] On the other hand, the physical situation of strong excitation is of high interest both for fundamental reasons and for device applications, where laser-induced structural changes of silver and gold nanoparticles in different media have been reported in Refs. 8–15.

High-intensity (strong) femtosecond laser irradiation of composite glasses that contain silver NPs has been found to display strong optical dichroism.[11,16] Essentially, the observed dichroism is a macroscopical consequence of the modified shapes of the NPs from spherical to prolate spheroids, which are oriented uniformly along the laser polarization direction.[17] In this context, the spectral changes of SP resonances are well understood with respect to the irradiation parameters;[18,19] however, the dynamical information regarding the NP shape transformation mechanisms (i.e., permanent changes in SP bands) remains as an interesting research topic.[12,20,21] Here we address the thermodynamical situation induced to the NP-glass system that allows the NP shape to get transformed in a rigid glass environment.

Studies so far have indicated that upon strong laser irradiation, conduction electrons of the NP can be emitted into the glass matrix along the laser polarization direction, thereby ionizing the NP.[21] The emitted electrons relax rapidly and they are trapped in the glass.[22] The remaining electrons equilibrate to a hot electronic distribution and heat up the NP lattice gradually. The electrodynamical and thermodynamical situation of the NP electrons and lattice can be investigated using the two-temperature model (2TM) in conjunction with the electronic band structure of the composite glass. The ionized, hot NP will no longer be stable, and due to the repulsive Coulomb forces, it ejects silver ions into the surrounding glass matrix.[22,23] These fast mechanisms were observed within the first 20 ps after the laser-pulse absorption, and a detailed analysis of these processes was investigated using femtosecond pulse-pair irradiation experiments.[21]

In this work, we present the dynamics happening on and around the NP in a longer time delay—until 1 ns—together with temperature modeling of the "NP-glass" system, which is named as three-temperature model (3TM) for convenience.[24] The experimental results of the long-time delays ($\Delta t > 20$ ps) suggest that a shell of glass surrounding the NP reaches transiently high temperatures that enable high diffusion mobility to the ejected silver ions. It is known from the results of ion implantation experiments that Ag^+ ions having 7–10 keV of energy can penetrate up to 10 nm deep in the glass,[25,26] if the glass is initially at room temperature. Additionally, the ionic penetration depths increase with the increasing glass temperature.[25,27] Discussing these results, it will be shown that a narrow zone of heat-affected glass results in high NP aspect ratios, while an extended shell of hot glass enables the emitted ions to go far away—reducing the NP volume and aspect ratio.

II. TEMPERATURE MODELING OF NANOPARTICLE-GLASS SYSTEM IN STRONG LASER EXCITATION

In this section, we discuss the spatiotemporal evolution of temperature in the NP-glass system after interaction with a single laser pulse. The excited NP electrons form a quasiequilibrated thermal electronic system as soon as the laser pulse is gone. Subsequently, the hot electrons cool down by sharing their energy with the lattice via electron-phonon coupling, thereby heating up the NP. The heat gained by the lattice can be calculated from the heat lost by the electrons using a 2TM compatible with the strong excitation regime, the details of which were described previously.[21]

The electronic temperature of a single silver NP (having a radius of $R=15$ nm) reaches around 10^4 K upon absorption of a 100 fs pulse with 0.5 $\mathrm{TW/cm^2}$ of intensity, which corresponds to an absorbed energy of around 3×10^{-13} J. Such a high electronic temperature is enough to heat up the Ag lattice to 2000 K. Afterwards, the electronic and lattice temperatures decrease together as the NP loses its energy to the surrounding "cold" glass. To account for the NP-glass thermodynamics, we need to consider the cooling of the NP together with the heating of the glass in the frame of the mentioned 3TM. On the NP-glass interface, the heat flow from the hot NP to the glass can be estimated step by step through concentrated spherical shells. After the first shell of the glass is heated, the following heat transfer deep into the glass can be described by the radial heat equation.

However, it is known for our excitation regime that the NP gets ionized by the emission of electrons, which consequently forces the NP to eject Ag^+ ions to the glass matrix through repulsive Coulomb forces. To destabilize (and destroy) a whole NP in our case of a rigid embedding medium, extreme irradiation conditions are required compared with the destruction of NPs in vacuum and fluids. The irradiation regime and the induced degree of ionization used in this work are far from causing destruction in NPs. It was shown that the NP loses a small part of its volume within 20 ps after the absorption of the laser pulse.[21] Compared to the small contribution of electron emissions and usual heat conduction (HC), ion emissions are definitely much more effective channels of rapid energy transfer from the NP, so that after the ion emissions one would expect high-temperature values for the glass in a larger range. Therefore, the above-described 3TM calculations are valid only for a "closed system," and we have to modify the 3TM by taking the fast contributions of ion emissions into account.

As ions are distinguishable classical particles, we can employ the Boltzmann distribution to designate the amount of energy carried by each emitted ion. In other words, the distribution plots the fractional number of emitted particles N_i as a function of their corresponding energy E_i. It was already mentioned that Ag^+ ions having 7–10 keV of energy can move up to a distance of 10 nm in glass at room temperature.[25,26] Therefore, we assume here that the emitted ions possess energy values from $E_i=0$ to 10 keV (i denotes a continuous set of energy states between these two values) with a maximum penetration depth of $d=10$ nm in glass. According to the exponential nature of the Boltzmann distribution, it is clear that a high fraction of ions will possess very less energy values (<1 keV); and as a result of this, they pileup in the immediate vicinity of the NP surface. On the other hand, only a few of the emitted ions can possess the maximum energy values. Additionally, the total number of ions $N=\Sigma_i N_i$ emitted from the NP depends on the strength of the laser irradiation. The area under the Boltzmann distribution for each energy state E_i gives a part of the total energy taken out by the ions. As the penetration depths of the ions depend on their initial energies, we can simply match these partial energy values with the spatial range $d=0-10$ nm of the emitted ions. As a result, we arrive at the spatial distribution of the energy that is transferred into the glass matrix. This energy distribution indicates that the highest amount of the energy emitted from the NP is located close to the surface of the NP; however, only small portions of the energy are transferred to the further spherical shells of the glass. At the end, we can convert the ionic energy into the glass temperature together with the calculation of the heat conduction in the glass.

Comprising these aspects, we can now calculate the spatial temperature distributions in the glass for different scenarios of heat transfer from the NP. Figure 1(a) shows the numerical calculations for several different scenarios. The dashed curve corresponds to the usual heat conduction from the NP at a time of $t=30$ ps after the NP lattice reaches its maximum temperature ($T_{lattice}$). Because of the huge difference in thermal diffusivities of Ag (123 $\mathrm{nm^2/ps}$) and glass (0.5 $\mathrm{nm^2/ps}$), any temperature gradient within the NP can be neglected. As the heat diffusivity of glass is very low, the heat transfer is observed to affect only a very narrow volume of glass surrounding the NP. This means that the cooling of the NP happens rather slowly by the heat conduction alone.

On the other hand, one can estimate from the above-mentioned Boltzmann distribution that 400 keV of energy will be taken out from the NP if approximately 300 ions are emitted by a single pulse irradiation. This energy corresponds to around 20% of the absorbed laser-pulse energy, which is transferred to a broad volume of glass by the ions within a short time. It should also be noted that a silver NP with a 15 nm radius has around 800.000 atoms, so that 300 ions correspond less than 0.1% of the total number of atoms in the NP. The radial temperature distribution of the NP-glass system for this case is given by the dash-dotted curve of Fig. 1(a), again at a time of 30 ps after the maximum $T_{lattice}$ is established. Comparing with the case of the pure heat conduction, it is clearly seen that ion emissions cool down the NP and heat up the glass much more effectively.

In this context, it is reasonable to expect that the temperature values of the glass matrix will depend strongly on the number of emitted ions N. As an illustration, we consider a stronger laser irradiation case that triggers higher number of ion emissions from the NP. It is estimated, for instance, that 50% of the absorbed laser-pulse energy is taken out from the NP when 800 ions are emitted into the glass. The radial temperature distribution in the glass for this case [the solid curve starting from 1000 K in Fig. 1(a)] shows that the NP loses half of its temperature, and the glass a few nm away from the NP surface reaches transiently higher temperatures than the NP itself. It is observed that a spherical zone of glass up to a distance of 10 nm from the NP surface is heated

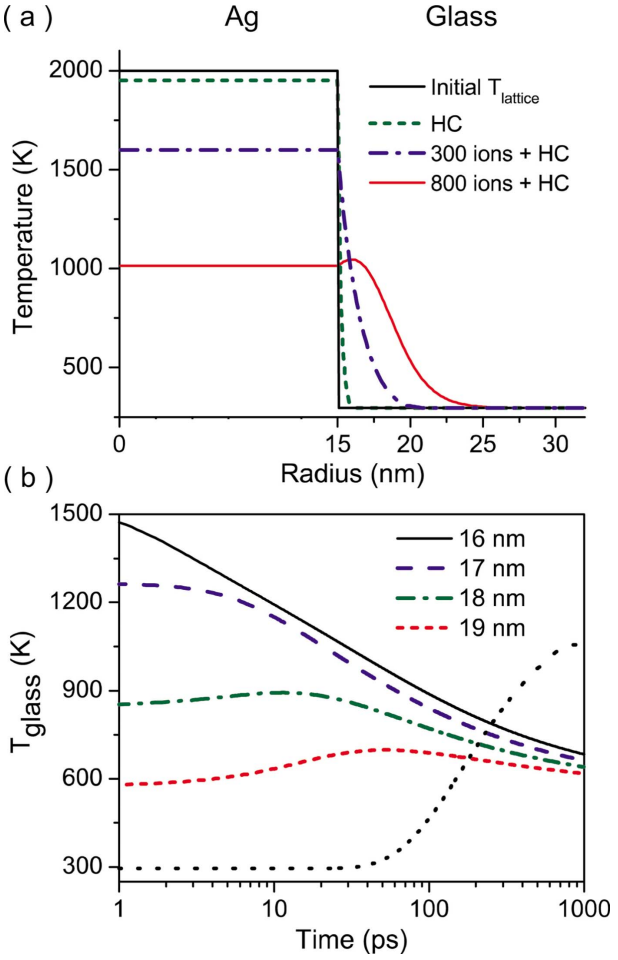

FIG. 1. (Color online) (a) Temperature distribution in the NP-glass system for different scenarios: pure HC at 30 ps after the initial $T_{lattice}$ is established, HC together with the emission of 300 and 800 ions again at the same time. (b) Temporal evolution of glass temperature for different spherical shells surrounding the NP ($R=15$ nm) for the cases of 800 ions+HC. The dotted curve represents the glass temperature at $R=16$ nm for the case of pure HC.

within a very short time owing to the high number of emitted ions.

Figure 1(b) shows the temporal evolution of glass temperatures in different radii away from the center of the NP for the case of 800 emitted ions with heat conduction. The temperature of the glass at $R=16$ and 17 nm are observed to have high-temperature values for short times because of the accumulation of a high number of emitted ions around these spherical shells. The temperature values decrease as the heat diffuses deep in the glass over time. The glass temperatures at $R=18$ and 19 nm start from lower values, as a comparably low number of ions are located there. It is observed that these shells reach their maximum temperature values later in time as the heat from inner shells arrives. The dotted curve starting from the room temperature (295 K) and reaching up to a value of 1050 K represents the glass temperature at $R=16$ nm for the case of pure heat conduction. One can see that in the absence of ion emissions, the formation of a soft glass volume around the NP takes very long time.

Summarizing this part we can say that ion emission is a fast-cooling mechanism for the NP extending the heated glass volume considerably compared with heat conduction alone. The temperature of the glass in a shell ≈ 3 nm around the NP surface exceeds the glass transition temperature of ≈ 850 K for the first 100 ps after interaction with one ultrashort laser pulse. This enables the softening of the glass, which is a necessary prerequisite for the NP shape transformations to take place.

III. EXPERIMENTAL

The samples studied here were prepared using the Ag-Na ion-exchange method for soda-lime glass with following annealing in H_2-reduction atmosphere.[28] This technique results in the formation of spherical silver NPs of 15 nm mean radius in a surface glass layer of 2–3 μm thickness. The NPs are sufficiently dispersed with a volume filling factor of 0.001; therefore, they can be treated as being isolated.

To investigate the laser-induced shape-transformation dynamics of the Ag NPs, we employ an experimental setup that generates time-delayed pulse pairs (wavelength $\lambda=400$ nm, pulse duration $\tau_{FWHM}=100$ fs, repetition rate 1 kHz) with equal energies.[21] One pulse can be delayed with respect to the other, producing pulse pairs with a variable time delay (Δt) in between. The pairs of pulses are focused on the sample to a spot size of about 100 μm, resulting in an energy density of 30 mJ/cm^2 per pulse. Moving the sample continuously on a motorized X-Y translation stage, a separate sample area is irradiated for each desired delay between pulse pairs. Through this way the temporal memory of the irradiations are stored in the sample by means of modified NP shapes.

It has been shown that only a very faint dichroism (1–2 nm separation between polarized plasmon bands) can be created when the NP is irradiated by a single laser pulse with the above given energy density.[19] This dichroism is due to the anisotropic distribution of a halo of small silver clusters surrounding the main NP, rather than a real prolate spheroidal shape of the NP. In the single-shot regime, one can generate an observable amount of separation between the polarized bands only at very high laser energy densities (around 300 mJ/cm^2). However, such high-intensity single-shot irradiation conditions transform the spherical shapes of the NPs into oblate spheroids.[17] It is, therefore, not possible in the single-shot regime to generate prolate spheroidal shapes. To investigate the shape transformation of spherical NPs into prolate spheroids, we need to be in the multishot irradiation conditions, where at least several tens of low-intensity laser pulses are allowed to hit a single spot on the sample. In this sense, to generate an optically observable amount of spectral separation between the bands, which is also needed for the determination of time-resolved effects (i.e., band shifts); the sample movement is arranged so that on average 300 pulse pairs (with an energy density of 30 mJ/cm^2 per pulse) hit one spot.

After the pulse-pair irradiations, the samples were annealed for 1 h at 200 °C in order to remove any possible laser-induced defects in the glass matrix.[22] Then the

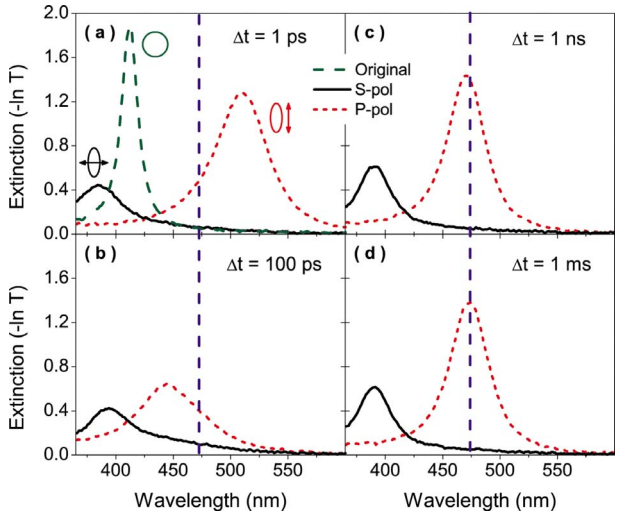

FIG. 2. (Color online) SP extinction bands of NPs resulting from pulse-pair irradiation experiments for different time delays. Dashed vertical lines are guides to the eyes, marking the central peak position of the P-polarized band of $\Delta t=1$ ms irradiation.

polarization-dependent SP extinction bands from each irradiated area (representing a single time delay Δt) are recorded by conventional transmission spectroscopy (Shimadzu 3100 UV/VIS/NIR spectrometer). These bands are then analyzed by the method of moments.[29]

IV. RESULTS

The original single surface plasmon band of the spherical silver NPs is split into two polarization-dependent bands [Fig. 2(a)] of electron oscillations: one parallel (P polarized) and one perpendicular (S polarized) to the long axis of the modified NP upon irradiation with linearly polarized laser pulses. The spectral gap between S- and P-polarized resonances depends strongly on the aspect ratio, namely, the ratio between the long to the short axes of the modified NP. Using the technique of pulse-pair irradiation, we found that the spectral gaps, and therefore also the NP shapes, depend strongly on the time delay Δt between the pulses of each pair. As an illustration to the effect of Δt on NP aspect ratios, some of the polarized spectra for several time delays are shown in Fig. 2.

Figure 2(a) shows the spectra from an area, which was irradiated by pulse pairs with a time delay of $\Delta t=1$ ps. It is clearly seen that the S- and P-polarized bands are well separated from each other. When the pulses are separated in time (e.g., $\Delta t=100$ ps), the resulting P-polarized band is observed to shift to shorter wavelengths with the central peak position at $\approx$450 nm [Fig. 2(b)]. The spectral position of the S-polarized band is almost the same with the $\Delta t=1$ ps irradiation. Considering the aspect ratios of the modified NPs for the 1 and 100 ps irradiation cases, it is apparent that the 1 ps irradiation results in a higher spectral gap, thereby higher aspect ratios for the NPs.

The spectra presented in Figs. 2(c) and 2(d) are obtained from irradiations with longer time delays. The time delay of $\Delta t=1$ ns results in a pretty interesting situation, which produces both S- and P-polarized bands almost at the same spectral positions with the ones of the 1 ms irradiation. Not only the positions of the 1 ns and 1 ms bands but also the bandwidths and band amplitudes are very similar to each other. The central peak position of the P-polarized band of the $\Delta t=1$ ms irradiation is marked with a dashed vertical line as a guide to the eyes for comparison. This line marks also the same spectral position in Figs. 2(a) and 2(b).

For a complete discussion of the NP shape modification dynamics, the full temporal evolution of the SP bands (from perfect overlapping of pulses until $\Delta t=1$ ns) will be presented in the following. For better visibility we will not show the complete spectra, but only their characteristic features in a parametrized form: employing the mentioned method of moments, we extract the central positions of the bands, the spectral gap between the bands, and the band integrals. The band centers, and, in particular, the difference of the positions of P- and S-polarized bands (called spectral gap), express the amount of dichroism. The spectral gap is a practical parameter considering the aspect ratios of the modified NPs. It decreases as the aspect ratio gets smaller (and vice versa), making it possible to comment on the shape transformation of NPs. The integrals of the plasmon bands are also important features for understanding of NP shape changes, as they contain information regarding band amplitudes and bandwidths at the same time. Physically, the temporal changes in band integrals (i.e., band areas) can be considered as absorption changes of the NP system; a decrease in the band integral represents a decrease in total amount of absorption and vice versa. This is in close correlation with the volume of the NPs.

Figure 3 displays the results of this parametrization for the whole accessible delay range. For comparison the results of the corresponding irradiation with an interpulse delay of $\Delta t=1$ ms are plotted as horizontal dashed lines. Figure 3(a) shows that the P-polarized band centers go below the P-polarized spectral position of the $\Delta t=1$ ms irradiation after a few picoseconds of time delay. The S-polarized band centers shift to longer wavelengths during the same time interval. Applying a second pulse to the disturbed NP after this time delay causes smaller spectral gaps than the $\Delta t=1$ ms irradiation. Both S- and P-polarized bands are observed to sit on plateaus around 430 and 450 nm, respectively, right after $\Delta t=20$ ps. This quasiconstant situation lasts until 100 ps. During this time interval the spectral gaps of the bands are at their minimum values of 20 nm [Fig. 3(b)]. After 100 ps of time delay, the polarized bands move away from each other again, reaching their long-term steady-state positions (obtained by the $\Delta t=1$ ms irradiation). It is seen that the spectral gaps increase rapidly (from 100 ps to 600 ps) from 20 to 55 nm, and then they reach their steady-state values at longer delays. The NP system reaches a long-term equilibrium from several hundred ps until 1 ns with slowed-down dynamics. The spectral positions of the bands at 1 ms delay are observed to be only a few nm away from their 1 ns positions.

The temporal features observed for the band centers in Fig. 3(a) are also expected to exist in the time dependence of band integrals. For the first 20 ps, Fig. 3(c) shows that the

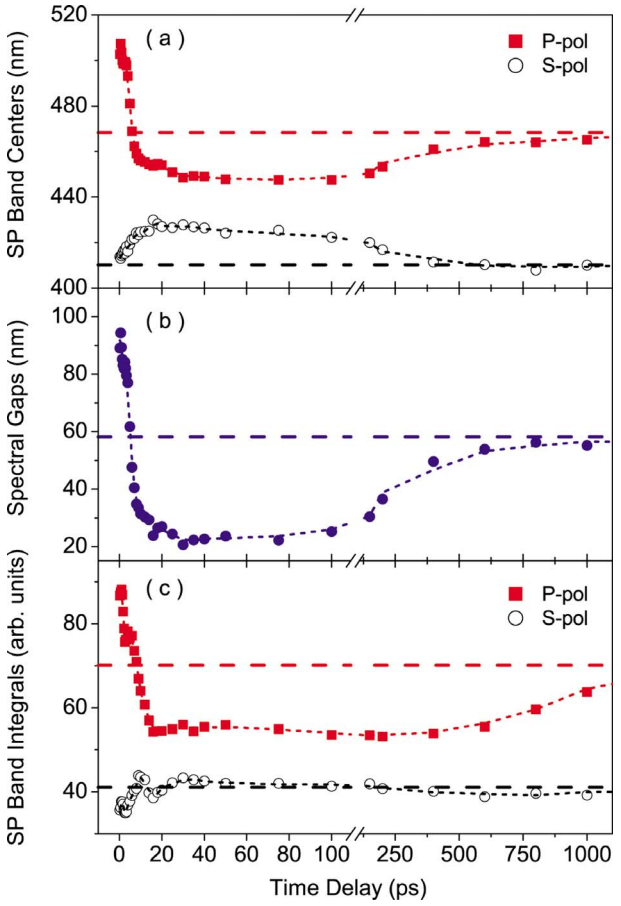

FIG. 3. (Color online) (a) SP band centers, (b) the corresponding spectral gaps, and (c) band integrals. The increments of the x axes change after the axes break. Horizontal dashed lines represent the positions of the corresponding band properties from the $\Delta t=1$ ms irradiation.

P-band integrals experience a sharp decrease while the S-band integrals show a slight increase. Reaching a nearly stable state around 20 ps, band integrals arrive at 100 ps with very little changes. After this time, again similarly to the dynamics of band centers, the band integrals move away from each other and reach a long-term equilibrium after 1 ns.

In general, the long-term results ($\Delta t>20$ ps) presented above can be characterized by two main regions: the first one is the time delay range roughly from 20 to 100 ps, where the spectral gaps remain nearly constant at their minimum values. The second region comprises delays from 100 ps to 1 ns, showing an increase of the spectral gaps up to their steady-state value. Since the small spectral gaps observed for $\Delta t<100$ ps are accompanied by decreased band integrals, it is obvious to attribute the smaller NP aspect ratios to partial dissolution of the NP. The latter might happen when the ions emitted by the second pulse in the already hot matrix can move too far away from the NP. The increasing NP aspect ratios and band integrals obtained for $\Delta t>100$ ps indicate that this partial dissolution gets less probable again, i.e., the average distance of the emitted ions from the NP decreases again. The following discussion will foster this idea by applying the temperature model introduced above to the concrete situation of delayed two-pulse irradiation of this study.

V. DISCUSSION

It is known from transmission electron microscope (TEM) images that roughly 60% of the NP volume is dissolved by ion emissions after applying 300 laser pulses with 0.5 TW/cm^2 to the NP.[24] Although there may be some differences in the absorption efficiency of an early pulse and a late pulse, which can result in different number of ion emissions from the NP, one can still consider an average efficiency for all pulses. As a result, we estimate in our case that the NP emits on average around 800 ions after the absorption of a single pulse. Additionally the TEM pictures of the irradiated NPs show that emitted ions can penetrate less than 10 nm in the glass from the surface of the NP.[24] These experimental findings strongly suggest considering the effect of ion emissions on the NP-glass system as it was introduced in Sec. II [see Fig. 1(a) for 800 emitted ions and Fig. 1(b)].

To account for our time-resolved results on the NP shape transformation dynamics, it is therefore of utmost importance to investigate the thermal situation of the glass in the vicinity of the NP, in the same manner as it was done in Sec. II, but for the case of pulse-pair irradiations. It is well known from the ion-implantation experiments that the diffusion ranges of the implanted ions increase with the increasing glass temperature.[25,27] Therefore, one can expect higher diffusion mobility for the emitted ions when the glass is already hot.

With this fact in mind, we have employed the glass temperature (T_{glass}) estimations of the single pulse irradiations [see Fig. 1(a)] and extended them by applying a time-delayed second pulse. In this case, the ions emitted by the second pulse experience a different T_{glass}, which depends strongly on the time delay between pulses. If the second pulse hits the NP shortly after the first one, so that the glass is still not heated by the first group of emitted ions, the second group of ions cannot have the benefit of high diffusion mobility. On the other hand, if the second pulse hits the NP when the glass is well heated by the first pulse effects (ion emissions and normal heat conduction), the second group of emitted ions can move far away from the main NP, causing the particle volume to shrink forever. Using the temperature-dependent penetration depth data of Ag ion implants into glass from Refs. 25 and 27, we can estimate the diffusion range of ions that are emitted into a glass of different temperatures. Afterwards the additional contribution of the second group of ions to the glass temperature is estimated as it was done in the single pulse case. Through this way, a new T_{glass} distribution for each desired Δt between pulse pairs can be calculated.

Figure 4 shows the radial temperature distribution in glass for several cases of pulse-pair irradiations having different time delays. The solid curve shows the case for the $\Delta t=0$ irradiation, which creates a high amplitude of glass temperature ($\approx$2500 K) around 2 nm away from the NP surface ($R=17$ nm) owing to the accumulation of a high number of emitted ions around this shell. Additionally, the heat-affected zone of the glass for this case of irradiation is observed to be pretty narrow. On the other hand, temporally separated pulse pairs create very different temperature distributions in the glass (see $\Delta t=30$, 70, 200, and 600 ps curves). It is clearly

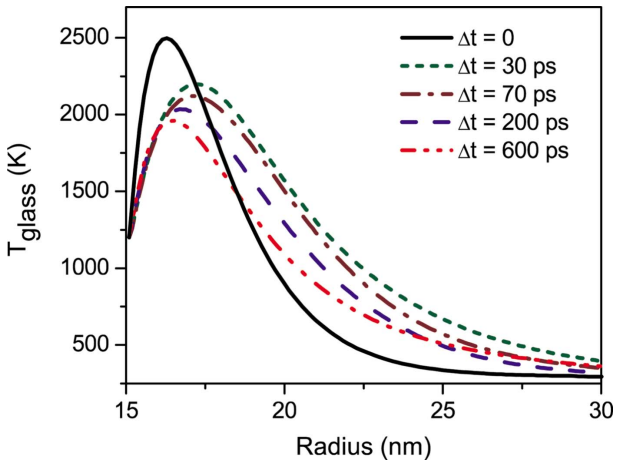

FIG. 4. (Color online) Temperature distribution in glass following the absorption of pulse pairs with different time delays. A broader volume of glass is heated for time delays of 30 and 70 ps compared to the longer delays.

seen that larger glass volumes are heated in all cases of irradiations with temporally separated pulses, and the maximum glass temperatures are achieved further away from the NP surface. Astonishingly, the largest volume of glass can be heated when the pulses are separated 30 ps (and 70 ps) from each other. As the time delay increases, the spherical range of the heated glass shrinks back toward the NP surface, approaching the situation that was obtained for $\Delta t=0$.

Now we can compare these estimations with our experimental results. It is clear that the simultaneous pulse-pair irradiation of the NP (i.e., with $\Delta t=0$) emits ions to a cold (not yet heated) glass matrix, which handicaps the diffusion ranges of the ions. Therefore, the ions are mostly located in the immediate vicinity of the NP and they heat up these concentrated glass shells. As the ions cannot travel too far away in the glass, they may diffuse back to and reaggregate with the main NP as soon as they are reduced by the trapped electrons. The other possibility for the reduced Ag atoms is that they form small silver clusters in the surroundings of the main NP, which are also observed by the TEM images of the modified NPs.[16,19] The experimental results demonstrate high spectral gaps [e.g., Figs. 2(a) and 3(a)], indicating high NP aspect ratios for very short-time delays. The corresponding total band integrals are also very high for short Δt [Fig. 3(c)], which means that the total volume of the NP is high and the emitted ions are not lost deep in the glass. Therefore, we can say that the estimations of the T_{glass} distribution for short-time delays, indicating a concentrated volume of heated glass, match the experimental results quite well.

The temporal interval of minimum NP aspect ratios and minimum SP band integrals observed in the experimental results between $\Delta t=20$ and 100 ps can also be explained in terms of the range of ionic mobility. It was shown in Fig. 4 that the maximum ranges of glass volume can be heated when the time delay between pulses is less than 100 ps. That means, the ions emitted by the second pulse can diffuse farther away from the NP, and they may stay there as the glass cools down. This of course will cause a reduction in the NP volume and thus hinders the generation of high NP aspect ratios. These ideas were tested by laser irradiations of Ag NPs on preheated glass samples, where we have reported complete dissolution of NPs when the global glass temperature is high enough.[24] This proves the significance of glass temperature as an indispensable but also a limiting component of the NP shape transformation mechanisms. The dissolution (or melting) of gold NPs suspended in water was also reported to take place within the same time scale of 100 ps following the intense laser-pulse excitation (comparable with the fluence employed in our studies).[12,13]

In this context, the experimental results showing a rapid fainting of dichroism in 20 ps strongly suggest that a mechanism of fast energy transfer across the nanoparticle-glass interface can be established by ion emissions [see Fig. 1(b)]. Summarizing the above given arguments, we can say that the reduction and the following precipitation of the silver ions with the NP are less probable until approximately 100 ps, because of the high ionic mobility and high glass temperatures in an increased glass volume during this time. If the laser irradiation is further intensified by increasing the energy of the pulses, the effect of NP dissolution will be much more drastic.

In the case when the second pulse follows the first pulse later and later in time (i.e., $\Delta t>100$ ps), the spatial range of the glass heated above some critical temperature gets reduced, which handicaps the ionic diffusion. Therefore the NP loses only less ions in the depth of the glass and higher NP aspect ratios can be realized. The gradual increase of the band integrals indicates that the overall absorption of the NP system (the volume of the main NP and the small silver clusters in the surroundings) increases in time. The details of these processes cover basically the reduction of the ions and their recombination with the main NP. The recombination processes happen in an anisotropic fashion because of the huge number of electrons trapped along the pole sides of the NP. This anisotropic electronic distribution is a product of laser-driven electron emissions, which define the memory of the NP reshaping mechanisms by means of ion reductions. The density of reduced ions (i.e., Ag atoms) along the pole sides of the NP is much higher than the reduced ions along the equator sides. Afterwards in time, the aggregated small silver clusters (i.e., Ag_2-Ag_8) join to the main NP.[22] This is a kind of Ostwald ripening process,[30] where large particles gain volume at the expense of the volume of small ones. Gradually (with the additional cycle of effects from the coming pulses) a growing NP aspect ratio is maintained along the pulse polarization direction. The time scale for these processes is clearly observed from Fig. 3(b), which shows the recombination of the silver clusters with the main NP to happen after 100 ps.

VI. CONCLUSIONS

Together with 3TM calculations, which have been modified to cover the heat transfer mechanisms with Ag ion emissions, we have found evidence that the temperature of the glass matrix surrounding the NP is of crucial importance for the NP shape modifications. An extended range of glass volume was shown to be heated within $\Delta t<100$ ps, which

proves that the emitted ions can diffuse in the depth of the glass, leaving behind a relatively small NP volume and aspect ratios. The heat-affected zone of the glass volume shrinks down as Δt exceeds 100 ps and the experimentally observed higher NP aspect ratios with higher NP volumes are realized. The maximum NP aspect ratios were observed when only a localized region of glass is heated (corresponds to the results of very short Δt), which gives enough freedom to the emitted ions to reshape the NP without letting them go too far away.

The theoretical estimations agree very well with the experimental results and show that the NP shape transformation mechanisms depend strongly on the thermal situation induced to the NP-glass system. A concentrated shell of glass around the NP with high transient temperatures is needed to create a high NP aspect ratio. The results indicated that the laser-induced shape transformation mechanisms of glass-embedded Ag NPs take place within 1 ns. The forthcoming pulses repeat the cycle of events summarized above on a step by step slightly modified NP.

ACKNOWLEDGMENTS

The authors thank Deutsche Forschungsgemeinschaft through SFB 418 for financial support and Codixx AG for the samples.

*uenal@mpi-halle.mpg.de

†Present address: Universität Hamburg, Bundesstraße 55, D-20146 Hamburg, Germany.

[1] U. Kreibig and M. Vollmer, *Optical Properties of Metal Clusters* (Springer, Berlin, 1995).

[2] S. A. Maier, M. D. Friedman, P. E. Barclay, and O. Painter, Appl. Phys. Lett. **86**, 071103 (2005).

[3] L. Yin, V. K. Vlasko-Vlasov, J. Pearson, J. M. Hiller, J. Hua, U. Welp, D. E. Brown, and C. W. Kimball, Nano Lett. **5**, 1399 (2005).

[4] J. Y. Bigot, V. Halte, J. C. Merle, and A. Daunois, Chem. Phys. **251**, 181 (2000).

[5] S. Link, C. Burda, M. B. Mohamed, B. Nikoobakht, and M. A. El-Sayed, Phys. Rev. B **61**, 6086 (2000).

[6] C. Voisin, D. Christofilos, P. A. Loukakos, N. Del Fatti, F. Vallee, J. Lerme, M. Gaudry, E. Cottancin, M. Pellarin, and M. Broyer, Phys. Rev. B **69**, 195416 (2004).

[7] A. Arbouet, C. Voisin, D. Christofilos, P. Langot, N. Del Fatti, F. Vallee, J. Lerme, G. Celep, E. Cottancin, M. Gaudry, M. Pellarin, M. Broyer, M. Maillard, M. P. Pileni, and M. Treguer, Phys. Rev. Lett. **90**, 177401 (2003).

[8] P. V. Kamat, M. Flumiani, and G. V. Hartland, J. Phys. Chem. B **102**, 3123 (1998).

[9] J. Bosbach, D. Martin, F. Stietz, T. Wenzel, and F. Trager, Eur. Phys. J. D **9**, 613 (1999).

[10] S. Link, Z. L. Wang, and M. A. El-Sayed, J. Phys. Chem. B **104**, 7867 (2000).

[11] M. Kaempfe, T. Rainer, K.-J. Berg, G. Seifert, and H. Graener, Appl. Phys. Lett. **74**, 1200 (1999); **77**, E459 (2000).

[12] A. Plech, V. Kotaidis, S. Gresillon, C. Dahmen, and G. von Plessen, Phys. Rev. B **70**, 195423 (2004).

[13] A. Plech, V. Kotaidis, M. Lorenc, and J. Boneberg, Nat. Phys. **2**, 44 (2006).

[14] T. Doppner, T. Fennel, P. Radcliffe, J. Tiggesbaumker, and K. H. Meiwes-Broer, Phys. Rev. A **73**, 031202(R) (2006).

[15] P. Zijlstra, J. W. M. Chon, and M. Gu, Nature (London) **459**, 410 (2009).

[16] M. Kaempfe, G. Seifert, K. J. Berg, H. Hofmeister, and H. Graener, Eur. Phys. J. D **16**, 237 (2001).

[17] A. Stalmashonak, G. Seifert, and H. Graener, Opt. Lett. **32**, 3215 (2007).

[18] S. Link and M. A. El-Sayed, Int. Rev. Phys. Chem. **19**, 409 (2000).

[19] A. Stalmashonak, A. Podlipensky, G. Seifert, and H. Graener, Appl. Phys. B: Lasers Opt. **94**, 459 (2009).

[20] G. Seifert, M. Kaempfe, K. J. Berg, and H. Graener, Appl. Phys. B: Lasers Opt. **71**, 795 (2000).

[21] A. A. Unal, A. Stalmashonak, G. Seifert, and H. Graener, Phys. Rev. B **79**, 115411 (2009).

[22] A. V. Podlipensky, V. Grebenev, G. Seifert, and H. Graener, J. Lumin. **109**, 135 (2004).

[23] T. Doppner, T. Fennel, T. Diederich, J. Tiggesbaumker, and K. H. Meiwes-Broer, Phys. Rev. Lett. **94**, 013401 (2005).

[24] A. Stalmashonak, A. A. Unal, H. Graener, and G. Seifert, J. Phys. Chem. C **113**, 12028 (2009).

[25] N. D. Skelland, J. Sharp, and P. D. Townsend, Nucl. Instrum. Methods Phys. Res. B **90**, 446 (1994).

[26] M. Dubiel, H. Hofmeister, E. Schurig, E. Wendler, and W. Wesch, Nucl. Instrum. Methods Phys. Res. B **166-167**, 871 (2000).

[27] N. D. Skelland and P. D. Townsend, J. Non-Cryst. Solids **188**, 243 (1995).

[28] K. J. Berg, A. Berger, and H. Hofmeister, Z. Phys. D: At., Mol. Clusters **20**, 309 (1991).

[29] G. G. Dyadyusha and A. A. Ishchenko, J. Appl. Spectrosc. **30**, 746 (1979).

[30] L. Ratke and P. W. Voorhees, *Growth and Coarsening: Ostwald Ripening in Material Processing* (Springer, Berlin, 2002).